

# Thickness dependence of ferrimagnetic compensation in amorphous rare-earth transition-metal thin films

Cite as: Appl. Phys. Lett. **113**, 172404 (2018); <https://doi.org/10.1063/1.5050626>

Submitted: 01 August 2018 . Accepted: 10 October 2018 . Published Online: 24 October 2018

Chung Ting Ma , Brian J. Kirby, Xiaopu Li, and S. Joseph Poon 



View Online



Export Citation



CrossMark

## ARTICLES YOU MAY BE INTERESTED IN

[An effect of capping-layer material on interfacial anisotropy and thermal stability factor of MgO/CoFeB/Ta/CoFeB/MgO/capping-layer structure](#)

Applied Physics Letters **113**, 172401 (2018); <https://doi.org/10.1063/1.5050486>

[Study of spin-orbit torque induced magnetization switching in synthetic antiferromagnet with ultrathin Ta spacer layer](#)

Applied Physics Letters **113**, 162402 (2018); <https://doi.org/10.1063/1.5045850>

[Ultrafast double magnetization switching in GdFeCo with two picosecond-delayed femtosecond pump pulses](#)

Applied Physics Letters **113**, 062402 (2018); <https://doi.org/10.1063/1.5044272>

## Applied Physics Letters

Mid-IR and THz frequency combs  
special collection

[Read Now!](#)



# Thickness dependence of ferrimagnetic compensation in amorphous rare-earth transition-metal thin films

Chung Ting Ma,<sup>1,a)</sup> Brian J. Kirby,<sup>2</sup> Xiaopu Li,<sup>1</sup> and S. Joseph Poon<sup>1</sup>

<sup>1</sup>Department of Physics, University of Virginia, Charlottesville, Virginia 22904, USA

<sup>2</sup>NIST Center for Neutron Research, National Institute of Standards and Technology, Gaithersburg, Maryland 20899, USA

(Received 1 August 2018; accepted 10 October 2018; published online 24 October 2018)

Magnetic compensation in ferrimagnets plays an important role in spintronic and magnetic recording devices. Experimental results have demonstrated a thickness dependence of the compensation temperature ( $T_{\text{comp}}$ ) in amorphous TbFeCo thin films. It was speculated that this thickness dependence originated from a variation in the short-range order. In this work, we have investigated the depth-resolved compositional and magnetization profiles using polarized neutron reflectometry. We find that although the composition is uniform across the film thickness, near the substrate interface, the magnetization exhibits a different temperature dependence from that of the rest of the sample. Monte Carlo simulations show that it is this difference in interfacial magnetization that causes the aforementioned thickness dependence of the compensation. These results demonstrate the critical role of the substrate interface in determining the magnetic properties of amorphous ferrimagnetic thin films for spintronic applications. *Published by AIP Publishing.*

<https://doi.org/10.1063/1.5050626>

Amorphous ferrimagnetic rare-earth-transition-metal (RE-TM) alloys have been investigated extensively for magneto-optical recording because of their perpendicular magnetic anisotropy (PMA).<sup>1–3</sup> The origin of the PMA was suggested to be the pair ordering or bond-orientation anisotropy induced from the growth of the amorphous thin films.<sup>4–8</sup> Apart from PMA, critical properties of the RE-TM alloys include the compensation temperature ( $T_{\text{comp}}$ ), where the moments of the two opposite RE and TM sublattices compensate each other. At  $T_{\text{comp}}$ , vanishing magnetization could be achieved for a range of compositions. Besides the composition, the ferrimagnetic compensation also depends on the film thickness. It was speculated that this thickness dependence of  $T_{\text{comp}}$  originates from variations in the short range order.<sup>9,10</sup> Thanks to this compensation, the RE-TM alloys continue to attract great interest for applications in high-density low-current spintronic devices and ultrafast magnetic recording.<sup>11–23</sup> For example, intrinsic exchange bias has been reported in compensated amorphous TbFeCo thin films.<sup>12</sup> The unidirectional exchange anisotropy is caused by a very large coercive field induced from a combination of PMA and reduced magnetization.

Another emerging area for RE-TM alloys is all-optical switching (AOS). AOS was first discovered in amorphous GdFeCo thin films using a circularly polarized laser by Stanciu *et al.*<sup>13</sup> The antiferromagnetic (AFM) coupling, the two opposite and very different sublattices, and PMA have been highlighted as the essential ingredients for designing AOS devices.<sup>18</sup> More recently, skyrmions were demonstrated to be driven under ultralow currents as topologically protected solitons.<sup>20,21</sup> The RE-TM system can host skyrmions because of its superexchanged sublattices.<sup>22</sup> The

dynamics of ferrimagnetic skyrmions have been theoretically studied close to the angular momentum compensation point.<sup>23</sup>

In the past, spin values and effective exchange interaction energies were extracted from the experimental results via simple mean-field analysis. With the growing power of modern computing, numerical modeling has become an essential tool to provide a deeper understanding of complex ferrimagnetic systems including both static and dynamic properties.<sup>24–26</sup> For magnetic modeling, several methods have been developed including Monte Carlo sampling,<sup>27–31</sup> the atomistic Landau-Lifshitz-Gilbert (LLG) algorithm,<sup>24,32,33</sup> and the micromagnetic Landau-Lifshitz-Bloch (LLB) algorithm.<sup>34,35</sup>

In this work, the thickness dependence of  $T_{\text{comp}}$  in amorphous TbFeCo thin films was investigated. Depth-resolved profiles of the composition and magnetization were measured through polarized neutron reflectometry (PNR). The composition is revealed to be uniform throughout the samples. Near the interface with the substrate, magnetization and  $T_{\text{comp}}$  were revealed to be different from those of the rest of the sample. Using Monte Carlo samplings, the magnetization profile was reproduced as a function of temperature to compare to PNR results. The total magnetization and  $T_{\text{comp}}$  calculated using this model are in good agreement with experiments. This result provides evidence that the interfacial region of RE-TM alloys exhibits different magnetic properties from the bulk region, which can have a significant influence on the development of ultra-thin devices.

Amorphous Tb<sub>26</sub>Fe<sub>64</sub>Co<sub>10</sub> thin films were prepared with thicknesses of 20 nm to 120 nm on thermally oxidized Si substrates by RF magnetron sputtering at room temperature. The base pressure was 0.07 mPa, and the deposition was carried out under an Ar pressure of 133 mPa by sputtering a single TbFeCo target. A 5 nm Ta capping layer was deposited

<sup>a)</sup>Author to whom correspondence should be addressed: [ctm7sf@virginia.edu](mailto:ctm7sf@virginia.edu)

on the samples to prevent oxidation. Thickness measurements were performed by the X-ray reflectivity (XRR) technique using Rigaku SmartLab (Note: Certain commercial equipment is identified in this paper to foster understanding. Such identification does not imply recommendation or endorsement by NIST nor does it imply that the materials or equipment identified are necessarily the best available for the purpose.). The magnetic properties at various temperatures were characterized using a vibrating sample magnetometer (VSM) option in a Quantum Design Versa Lab system.

**Polarized neutron reflectometry (PNR) measurements were conducted using the PBR beamline at the NIST Center for Neutron Research.** Temperature-dependent PNR measurements were performed in a 3 T in-plane field. The non-spin-flip reflectivities  $R^{++}$  and  $R^{--}$  were measured as functions of wavevector transfer  $Q$  along the sample surface normal direction. Data reduction and model fitting were performed with the *reductus*<sup>36</sup> and Refl1D software packages,<sup>37</sup> respectively. Via modeling, we determined the depth dependence of the neutron scattering length density,  $\rho$ , which has both a nuclear component (related to the nuclear composition of the sample) and a magnetic component (proportional to the in-plane magnetization).<sup>38</sup> The reported uncertainties correspond to one standard deviation, with the exception of PNR fitting parameters, for which we use two standard deviations.

VSM was used to measure the temperature dependence of magnetization of TbFeCo thin films following a field and temperature treatment. First, the temperature of the samples was raised from room temperature to 375 K in zero magnetic field. Second, a magnetic field of 3 T was applied in the out-of-plane direction to fully magnetize the samples. Third, the magnetic field was removed (the sample magnetization was maintained due to the strong PMA). Following those steps, the temperature-dependent magnetization was measured from 375 K to 200 K in zero magnetic field, as shown in Fig. 1(a).

From Fig. 1(a), the remanent magnetization decreases as temperature decreases for all thicknesses. It goes from positive at 375 K to negative at 200 K. At 375 K, since the samples are fully magnetized in the 3 T applied field, samples of all thicknesses have positive remanent magnetization. As the temperature cools down from 375 K, the Tb sublattice magnetization progressively increases in magnitude while retaining a negative orientation with respect to the applied field. At  $T_{\text{comp}}$ , the magnetic moments of the antiferromagnetically

coupled Tb and FeCo sublattices completely cancel and the total magnetization of the sample goes to zero. Below  $T_{\text{comp}}$ , the total moment of the Tb sublattice is larger than the total moment of the FeCo sublattice, and the net magnetization becomes negative. As shown in Figs. 1(a) and 1(b),  $T_{\text{comp}}$  increases for samples with a higher thickness. This implies a greater weight of FeCo sublattice moment in thinner samples. In Fig. 1(b),  $T_{\text{comp}}$  is plotted as a function of thickness.  $T_{\text{comp}}$  of 20 nm, 40 nm, 80 nm, and 120 nm is  $278 \pm 5$  K,  $336 \pm 1.5$  K,  $358 \pm 1.5$  K, and  $372 \pm 2.5$  K, respectively. As the thickness increases, the increment of  $T_{\text{comp}}$  reduces and begins to level off. This implies that the thickness dependence may originate from an interfacial effect. The variations in error measurements are primarily due to background noise in the magnetic moment measurement. The  $T_{\text{comp}}$  of the 120 nm thick film, being close to upper bound of the accessible temperature range (375 K), also increases the error in the experiment.

To investigate the origin of thickness dependence of  $T_{\text{comp}}$  in TbFeCo thin films, we employed PNR to measure the compositional and magnetic depth profiles of magnetization of the samples. Figure 2(a) shows the model-fitted temperature dependent scattering data for the 80 nm TbFeCo plotted as spin asymmetry (the difference in  $R^{++}$  and  $R^{--}$  divided by the sum). The results demonstrate a clear temperature dependence due to the ferrimagnetic nature of this film. Figure 2(b) presents the scattering length density profiles corresponding to the fits in (a). The nuclear profile shows clear steps associated with the  $\text{SiO}_2$  substrate, TbFeCo film, and Ta capping layer. Notably, the data are consistent with a TbFeCo layer that is compositionally uniform throughout its thickness, evident by the flat nuclear profile. Conversely, the data cannot be fitted using a uniform magnetic profile. Two magnetic sublayers are required, one 5 nm thick at the substrate interface and another corresponding to the remainder of the film thickness. Interestingly, the magnetic scattering length densities of these two regions exhibit different temperature dependencies. Figure 2(c) summarizes the temperature-dependent magnetic profiles of the two regions in units of magnetization. From 100 K to 300 K, the magnetization of the interfacial region increases with temperature.  $T_{\text{comp}}$  of the interfacial region is about 100 K. On the other hand, the magnetization of the rest of the sample decreases as temperature increases, demonstrating that  $T_{\text{comp}}$  of the rest of the sample is above 300 K. Similar temperature-dependent behavior of the magnetization is also observed in the 20 nm film, which is provided in the [supplementary material](#). The origin of this interfacial layer is

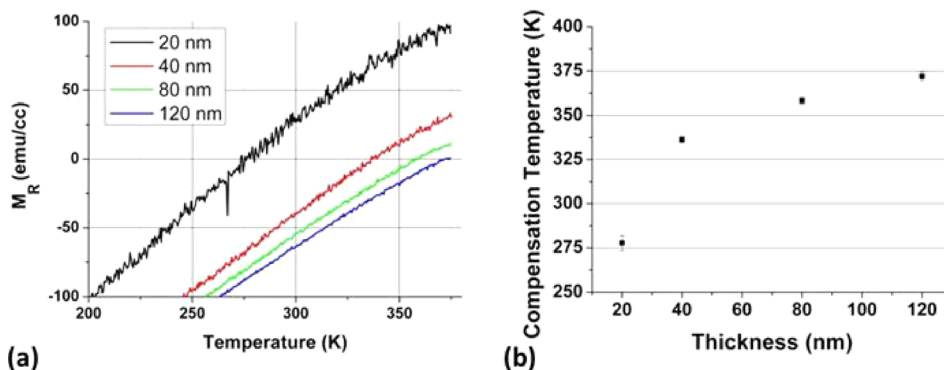


FIG. 1. (a) Temperature dependence of remanent magnetization ( $M_R$ ) of 20 to 120 nm amorphous  $\text{Tb}_{26}\text{Fe}_{64}\text{Co}_{10}$  thin films from 200 K to 375 K. (b) Thickness dependence of the compensation temperature in amorphous  $\text{Tb}_{26}\text{Fe}_{64}\text{Co}_{10}$  thin films.

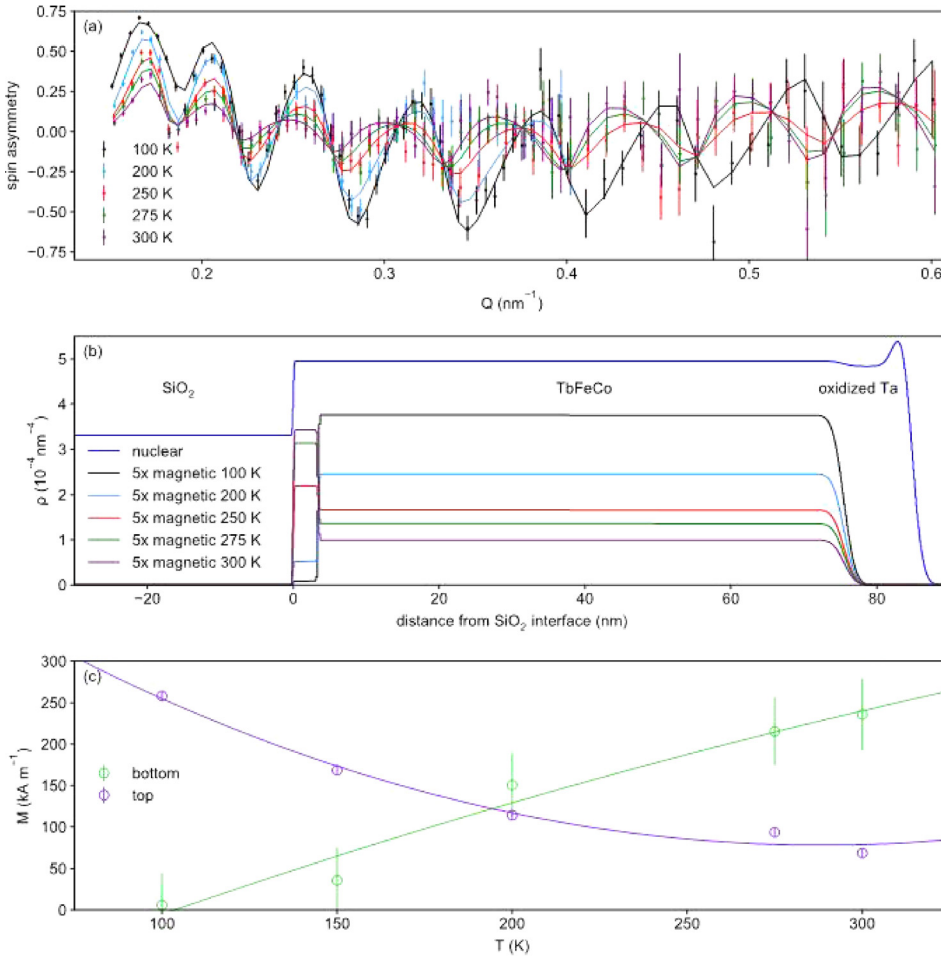


FIG. 2. (a) Temperature dependent fitted scattering data of the 80 nm amorphous Tb<sub>26</sub>Fe<sub>64</sub>Co<sub>10</sub> thin film. (b) The scattering length density profiles of the 80 nm amorphous Tb<sub>26</sub>Fe<sub>64</sub>Co<sub>10</sub> thin film. (c) Magnetization vs. temperature for the bottom 5 nm (interfacial region) and top (the rest of the sample).

likely due to variations in short range order of GdFeCo near the interface. Further experiments are needed to reveal the exact origin.

Based on the PNR results, the Monte Carlo Metropolis sampling method<sup>39</sup> is employed to reproduce the magnetization as a function of temperature for both regions. Classical atomistic spin Hamiltonian is utilized to find the ground state of the system. Values of exchange couplings ( $J_{ij}$ ) were taken from Ostler *et al.*<sup>24</sup> In this simulation, amorphous Tb<sub>x</sub>(FeCo)<sub>1-x</sub> is modeled using a chemically disordered face-centered cubic (FCC) lattice. As such, 32 × 32 × 32 atoms are randomly distributed in FCC cells. The magnetization vs. temperature is simulated through Monte Carlo samplings in 25 K temperature intervals from 1600 K to 0 K. Figure 3 presents the simulated magnetization vs. temperature of the interfacial

region and the bulk region. In Fig. 3(a), the  $T_{\text{comp}}$  of the 5 nm interfacial is found to be near 125 K. On the other hand, Fig. 3(b) shows that the  $T_{\text{comp}}$  of the rest of the sample is between 375 K and 400 K.

Using the magnetization vs. temperature results from simulations, an average magnetization model in Eq. (1) is employed to determine the temperature dependence of an entire sample

$$M_{\text{ave}}(T) = \frac{M_{\text{int}}(T)t_{\text{int}} + M_{\text{rest}}(T)t_{\text{rest}}}{t_{\text{int}} + t_{\text{rest}}}, \quad (1)$$

where  $M_{\text{ave}}$  is the total magnetization,  $M_{\text{int}}$  is the magnetization of the interfacial region,  $M_{\text{rest}}$  is the magnetization of the rest of the sample,  $t_{\text{int}}$  is the thickness of the interfacial region, and  $t_{\text{rest}}$  is the thickness of the rest of the sample.

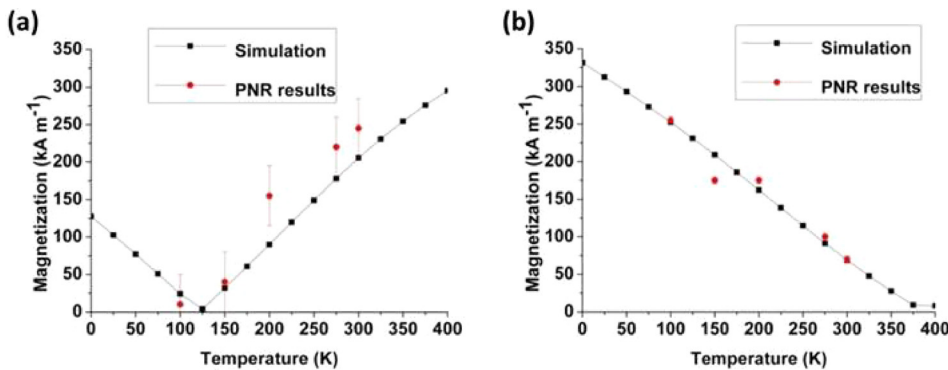


FIG. 3. (a) Simulated magnetization as a function of temperature of the bottom 5 nm (interfacial region) based on PNR results. (b) Simulated magnetization as a function of temperature of the top region (rest of the sample) based on PNR results. The error of PNR results in (b) is much smaller than that in (a).

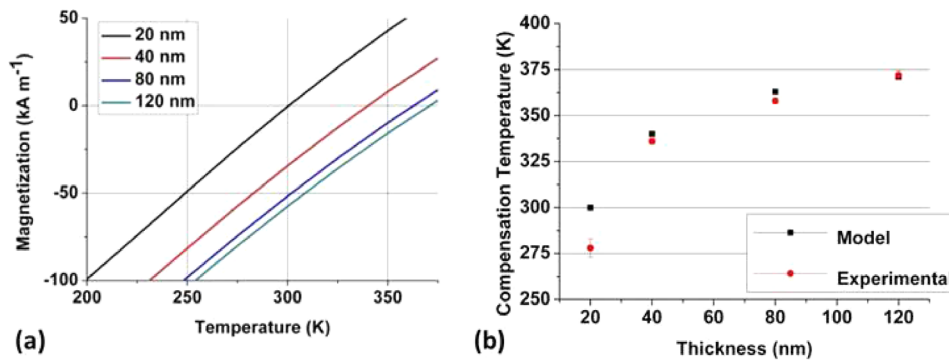


FIG. 4. (a) Temperature dependence of magnetization of the 20 to 120 nm sample from 200K to 375K using the average magnetization model from Eq. (1). (b) Thickness dependence of the compensation temperature in amorphous Tb<sub>26</sub>Fe<sub>64</sub>Co<sub>10</sub> thin films using the total magnetization model.

In order to be comparable with experimental results presented in Fig. 1, the calculation of  $M_{\text{ave}}$  assumes that the FeCo sublattice is aligned in the positive direction, while the Tb sublattice is aligned in the negative direction. Figure 4(a) presents  $M_{\text{ave}}$  calculated using Eq. (1) as a function of temperature for 20-nm to 120-nm films. The results show consistent temperature dependence of  $M_{\text{ave}}$  for all thicknesses in comparison to experiments. Figure 4(b) shows the thickness dependence of  $T_{\text{comp}}$  using the total magnetization model. In this model,  $T_{\text{comp}}$  of 20 nm, 40 nm, 80 nm, and 120 nm is 300 K, 340 K, 363 K, and 371 K, respectively. In comparison, the experimental  $T_{\text{comp}}$  of 20 nm, 40 nm, 80 nm, and 120 nm is  $278 \pm 5$  K,  $336 \pm 1.5$  K,  $358 \pm 1.5$  K, and  $372 \pm 2.5$  K, respectively. This provides strong evidence that the existence of the interfacial region leads to the thickness dependence of  $T_{\text{comp}}$ .

In summary, the thickness dependence of magnetization and compensation temperature is investigated in amorphous TbFeCo thin films. Although the composition is uniform across the film thickness, an interfacial region of about 5 nm is revealed by polarized neutron reflectometry exhibiting different magnetic properties from the rest of the sample. Using a total magnetization model coupled with atomistic simulation, it is confirmed that the interfacial region leads to the thickness dependence of compensation temperature in TbFeCo thin films. The origin of this rather thick interfacial region is apparently due to the formation of a different amorphous phase near the interface, resulting in changes of short range order of the amorphous TbFeCo film. Further experiments are needed to identify the exact origin of the interfacial region. Nevertheless, the existence of the interfacial region in RE-TM thin films underscores potential challenges in developing ultra-thin RE-TM spintronic devices.

See [supplementary material](#) for the PNR results of the 20 nm TbFeCo film.

This work was partially supported by DARPA Topological Excitations in Electronics Program.

<sup>1</sup>F. Tanaka, S. Tanaka, and N. Imamura, *Jpn. J. Appl. Phys., Part 1* **26**, 231 (1987).

<sup>2</sup>P. Hansen, C. Clausen, G. Much, M. Rosenkranz, and K. Witter, *J. Appl. Phys.* **66**, 756 (1989).

<sup>3</sup>S. Tsunashima, "Magneto-optical recording," *J. Phys. D: Appl. Phys.* **34**, R87 (2001).

<sup>4</sup>A. G. Dirks and H. J. Leamy, *Thin Solid Films* **47**, 219 (1977).

<sup>5</sup>H. J. Leamy and A. G. Dirks, *J. Appl. Phys.* **49**, 3430 (1978).

<sup>6</sup>V. G. Harris, K. D. Aylesworth, B. N. Das, W. T. Elam, and N. C. Koon, *Phys. Rev. Lett.* **69**, 1939 (1992).

<sup>7</sup>V. G. Harris and T. Pokhil, *Phys. Rev. Lett.* **87**, 67207 (2001).

<sup>8</sup>N. Anunniwat, M. Ding, S. J. Poon, S. A. Wolf, and J. Lu, *J. Appl. Phys.* **113**, 43905 (2013).

<sup>9</sup>B. Hebler, A. Hassdenteufel, P. Reinhardt, H. Karl, and M. Albrecht, *Front. Mater.* **3**, 8 (2016).

<sup>10</sup>A. V. Svalov, O. A. Adanakova, V. O. Vas'kovskiy, K. G. Balymov, A. Larrañaga, G. V. Kurlyandskaya, R. Domingues Della Pace, and C. C. Plá Cid, *J. Magn. Magn. Mater.* **459**, 57 (2018).

<sup>11</sup>N. Nishimura, T. Hirai, A. Koganei, T. Ikeda, K. Okano, Y. Sekiguchi, and Y. Osada, *J. Appl. Phys.* **91**, 5246 (2002).

<sup>12</sup>X. Li, C. T. Ma, J. Lu, A. Devaraj, S. R. Spurgeon, R. B. Comes, and S. J. Poon, *Appl. Phys. Lett.* **108**, 012401 (2016).

<sup>13</sup>C. D. Stanciu, F. Hansteen, A. V. Kimel, A. Kirilyuk, A. Tsukamoto, A. Itoh, and T. Rasing, *Phys. Rev. Lett.* **99**, 47601 (2007).

<sup>14</sup>A. Kirilyuk, A. V. Kimel, and T. Rasing, *Rev. Mod. Phys.* **82**, 2731 (2010).

<sup>15</sup>A. Hassdenteufel, B. Hebler, C. Schubert, A. Liebig, M. Teich, M. Helm, M. Aeschlimann, M. Albrecht, and R. Bratschitsch, *Adv. Mater.* **25**, 3122 (2013).

<sup>16</sup>C. Schubert, A. Hassdenteufel, P. Matthes, J. Schmidt, M. Helm, R. Bratschitsch, and M. Albrecht, *Appl. Phys. Lett.* **104**, 82406 (2014).

<sup>17</sup>S. Mangin, M. Gottwald, C.-H. Lambert, D. Steil, V. Uhlir, L. Pang, M. Hehn, S. Alebrand, M. Cinchetti, G. Malinowski, Y. Fainman, M. Aeschlimann, and E. E. Fullerton, *Nat. Mater.* **13**, 286 (2014).

<sup>18</sup>A. V. Kimel, *Nat. Mater.* **13**, 225 (2014).

<sup>19</sup>C.-H. Lambert, S. Mangin, B. S. D. Ch, S. Varaprasad, Y. K. Takahashi, M. Hehn, M. Cinchetti, G. Malinowski, K. Hono, Y. Fainman, M. Aeschlimann, and E. E. Fullerton, *Science* **345**, 1337 (2014).

<sup>20</sup>X. Z. Yu, N. Kanazawa, W. Z. Zhang, T. Nagai, T. Hara, K. Kimoto, Y. Matsui, Y. Onose, and Y. Tokura, *Nat. Commun.* **3**, 988 (2012).

<sup>21</sup>J. Sampaio, V. Cros, S. Rohart, A. Thiaville, and A. Fert, *Nat. Nanotechnol.* **8**, 839 (2013).

<sup>22</sup>J. C. T. Lee, J. J. Chess, S. A. Montoya, X. Shi, N. Tamura, S. K. Mishra, P. Fischer, B. J. McMorrin, S. K. Sinha, E. E. Fullerton, S. D. Kevan, and S. Roy, *Appl. Phys. Lett.* **109**, 022402 (2016).

<sup>23</sup>S. K. Kim, K. J. Lee, and Y. Tserkovnyak, *Phys. Rev. B* **95**, 140404 (2017).

<sup>24</sup>T. A. Ostler, R. F. L. Evans, R. W. Chantrell, U. Atxitia, O. Chubykalo-Fesenko, I. Radu, R. Abrudan, F. Radu, A. Tsukamoto, A. Itoh, A. Kirilyuk, T. Rasing, and A. Kimel, *Phys. Rev. B* **84**, 024407 (2011).

<sup>25</sup>I. Radu, K. Vahaplar, C. Stamm, T. Kachel, N. Pontius, H. A. Dürr, T. A. Ostler, J. Barker, R. F. L. Evans, R. W. Chantrell, A. Tsukamoto, A. Itoh, A. Kirilyuk, T. Rasing, and A. V. Kimel, *Nature* **472**, 205 (2011).

<sup>26</sup>C. T. Ma, X. Li, and S. J. Poon, *J. Magn. Magn. Mater.* **417**, 197 (2016).

<sup>27</sup>E. Ising, *Z. Phys.* **31**, 253 (1925).

<sup>28</sup>S. H. Charap, P.-L. Lu, and Y. He, *IEEE Trans. Magn.* **33**, 978 (1997).

<sup>29</sup>E. Restrepo-Parra, J. Restrepo, J. F. Jurado, C. Vargas-Hernandez, and J. C. Riano-Rojas, *IEEE Trans. Magn.* **45**, 5180 (2009).

<sup>30</sup>J. D. Earl and M. W. Deem, *Phys. Chem. Chem. Phys.* **7**, 3910 (2005).

<sup>31</sup>A. Kone and D. A. Kofke, *J. Chem. Phys.* **122**, 206101 (2005).

<sup>32</sup>T. L. Gilbert and J. M. Kelly, in *Conference on Magnetism Magnetic Materials*, Pittsburgh, PA, June 14–16, 1955 (American Institute of Electrical Engineers, New York, 1955), p. 253.

- <sup>33</sup>R. F. L. Evans, W. J. Fan, P. Chureemart, T. A. Ostler, M. O. A. Ellis, and R. W. Chantrell, *J. Phys. Condens. Matter* **26**, 103202 (2014).
- <sup>34</sup>D. A. Garanin, *Phys. Rev. B* **55**, 3050 (1997).
- <sup>35</sup>R. F. L. Evans, D. Hinzke, U. Atxitia, U. Nowak, R. W. Chantrell, and O. Chubykalo-Fesenko, *Phys. Rev. B* **85**, 014433 (2012).
- <sup>36</sup>B. Maranville, W. Ratcliff II, and P. Kienzle, *J. Appl. Cryst.* **51**, 1500 (2018).
- <sup>37</sup>B. J. Kirby, P. A. Kienzle, B. B. Maranville, N. F. Berk, J. Krycka, F. Heinrich, and C. F. Majkrzak, *Curr. Opin. Colloid Interface Sci.* **17**, 44 (2012).
- <sup>38</sup>C. F. Majkrzak, K. V. O'Donovan, and N. F. Berk, *Neutron Scattering from Magnetic Materials* (Elsevier, Amsterdam, 2006), pp. 397–471.
- <sup>39</sup>N. Metropolis, A. W. Rosenbluth, M. N. Rosenbluth, A. H. Teller, and E. Teller, *J. Chem. Phys.* **21**, 1087 (1953).